Appl. Phys. B 68, 1031–1038 (1999) / DOI 10.1007/s003409900023

Applied Physics B
Lasers
and Optics

Adaptive correlation filters for speckle patterns in photorefractive crystals

A.A. Kamshilin[1], K. Paivasaari[1], N.I. Nazhestkina[1], V.V. Prokofiev[1], S. Ashihara[2], Y. Iida[2], T. Shimura[2], K. Kuroda[2]

[1] Department of Physics, University of Joensuu, P.O. Box 111, FIN-80101, Joensuu, Finland
[2] Institute of Industrial Science, University of Tokyo, Roppongi, Minato-ku, Tokyo 106, Japan
(Fax: +358-13/251-3290, E-mail: alexei.kamshilin@joensuu.fi)

Received: 27 November 1998/Revised version: 26 January 1999/Published online: 12 April 1999

Abstract. The experimental study of the in-plain vibration of the speckle pattern in photorefractive GaP and BTO crystals using the polarization self-modulation effect are presented. The simple model based on the propagation of the Gaussian beam through the crystal with recorded space-charge field is proposed to explain main features of the experiment. It is shown that these results allow designing a linear sensor of the speckle-pattern displacement in an effective way. The optical system is very simple and does not include any reference or readout beam. The sensitivity of this system is the same as that of an interferometer.

PACS: 42.65.H; 42.70.N; 42.30.M

It is well known that coherent light scattered by any object produces the speckle patterns, whose structure varies while the object suffers any distortions, particularly, displacements or vibrations. Therefore, the analysis of the speckle pattern variations allows us to get information about an object's dynamics. However, the random character of the speckle pattern's intensity distribution makes the solution of this problem technically difficult. It is necessary to record an average intensity distribution of the vibrating speckle pattern and then the correlation with the instant intensity distribution should be estimated. The search for an adequate medium, which allows fast recording and correlation analysis of a speckle pattern, is an important task. The photorefractive crystals are promising candidates for solving this task. A distinguishing feature of these crystals from other materials for optical data recording is their ability to record and update the input information continuously. Particularly, the adaptation of the photorefractive crystals to slowly varying environmental changes is naturally implemented. This feature has been successfully used in the adaptive interferometers based on photorefractive crystals [1–4]. Recording and analysis of speckle patterns in photorefractive crystals have been also demonstrated. The methods involved are the double-exposure recording with following readout of the information by additional beam and analysis of the Young fringes [5, 6]; self-diffraction of the speckle pattern recorded in a photorefractive crystal under dc electric field [7]; self-diffraction of the speckle pattern from a double-phase-conjugate mirror [8]; self-diffraction of the speckle pattern from gratings recorded due to the fanning effect [9]. All the above-mentioned methods are based on light diffraction from the spatially non-uniform refractive index caused by the recorded speckle pattern. Any speckle-pattern displacement from its average position leads to variation of the diffraction efficiency if the displacement occurs faster than the crystal response time.

Another approach to speckle-pattern displacement measurements was proposed to exploit a non-steady-state photo-EMF-generation observed in photorefractive crystals [10, 11]. In this method, the speckle pattern produces an internal electric field of the spatially redistributed charges and the fast displacement of the input speckle pattern results in the generation of the electric current in the crystal. Recently an alternative method of the speckle-pattern-displacement measurement was proposed, which does not use either diffraction or photo-EMF [12]. It is based on the polarization self-modulation effect that manifests itself in the spatial modulation of the polarization state of the speckle field transmitted through the photorefractive crystals. Here the speckle pattern displacement results in the polarization state modulation, which can be readily transferred into the intensity modulation by means of a polarization analyzer. In this paper we present experimental results of the studies on in-plane vibrations of the speckle pattern using the polarization self-modulation. Experiments were carried out using photorefractive $Bi_{12}TiO_{20}$ and GaP crystals. To explain the main features of the experiments we propose a simple heuristic model based on the propagation of a Gaussian beam through a crystal with recorded space-charge field.

1 Experiment

Experiments were performed using an optical setup schematically shown in Fig. 1. The setup is very simple and easily adjustable. The laser beam derived from a conventional

Dedicated to Prof. Dr. Eckard Krätzig on the occasion of his 60th birthday.

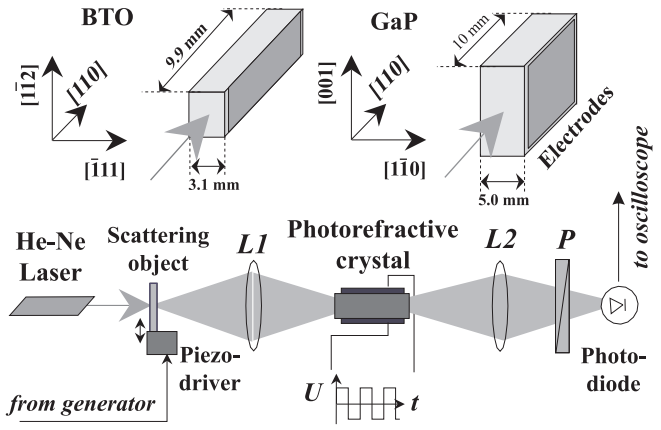

Fig. 1. Crystal orientation, dimensions, and schematic of the optical setup used in experiments. Light propagates along the [110] crystallographic axis in both BTO and GaP. External electric field vector is parallel to the [$\bar{1}$11] axis in BTO and [1$\bar{1}$0] axis in GaP. L1 and L2 are lens systems for light gathering and focusing in the optical setup. P is the polarization analyzer

He-Ne laser is scattered by a rough surface under study. Both transmission and reflection geometry has been used, however, for the sake of simplicity, only the transmission geometry is shown in Fig. 1. Scattered light is collected by a lens L1 into a photorefractive crystal. Average transverse size of the speckles is defined by the F-number of the lens. It is 3.7 μm in the experiments with GaP crystal and 3.0 μm in the experiments with $Bi_{12}TiO_{20}$ (BTO) crystal. All light transmitted through the crystal is collected by a lens L2 into a conventional photodiode after passing through a polarization analyzer, P. The photodiode's current proportional to the light intensity is measured by either oscilloscope or lock-in amplifier. During the experiment, the scattering object was excited by a piezo-electric transducer producing a lateral small-amplitude-displacement of the speckle pattern. The displacement vector is parallel to the external electric field applied to the photorefractive crystal.

Two photorefractive crystals of different symmetry were used in the experiments. BTO crystal (symmetry class 23) was grown in the Department of Physics, University of Joensuu, Finland. Semi-insulating GaP crystal (symmetry class $\bar{4}3m$) was grown in Sumitomo Metal Mining Co., Japan. The BTO sample was cut so that the light propagates along the [110] crystallographic axis and the external electric field vector is parallel to the [$\bar{1}$11] axis. The sample dimensions are $3.3 \times 4.3 \times 9.9$ mm, where the first measurement is along the electric-field vector and the third one is along the light propagation direction. The orientation of GaP sample was different: the light propagates along the [110] axis, but the electric field is applied along the [1$\bar{1}$0] axis. This sample has the size of $5.0 \times 10.0 \times 10.0$ mm. The silver and gold evaporated electrodes provided the application of the external electric field to the BTO and GaP samples, respectively. We applied a bipolar alternating voltage of a square-wave form with a repetition rate, that can be varied from 0.1 Hz to 200 Hz.

1.1 Intensity modulation of the non-stationary speckle pattern

We have observed that the total intensity of the speckle pattern transmitted through the crystal–polarization analyzer pair is modulated in time at the same frequency as the speckle pattern's oscillations. Therefore, linear sensing of the lateral displacement of the speckle pattern is achieved in our setup. As an example, we show in Fig. 2 an oscilloscope trace of the photodiode current (upper trace (a)). The middle trace (b) corresponds to the voltage applied to the piezo-driver, which is assumed proportional to the speckle-pattern displacement. The lower trace (c) is the voltage applied to the photorefractive crystal. All these traces were recorded simultaneously. As seen from Fig. 2, the transmitted light power is modulated almost in phase with the driving voltage during the negative semi-cycle of the voltage applied to the crystal whereas it is almost out of phase during the positive semi-cycle. Small dephasing between the driving voltage and light-power modulation is due to electromechanical features of our particular piezo-driver. Sharp peaks of the photodiode current in trace (a) are caused by the finite slew rate of the applied voltage, which is seen from trace (c). The oscilloscope traces shown in Fig. 2 were recorded using the GaP sample. Similar traces were obtained with the BTO sample. No transmitted light modulation has been detected without a ac field applied to the crystal even in the case of large vibration amplitude of a speckle pattern. Moreover, there is no modulation if the polarization analyzer is uninstalled.

The modulation of the transmitted intensity primarily depends on the vibrating amplitude of the scattering object. Dependencies of the intensity modulation depth, which is defined as the ratio of the modulation amplitude to the mean intensity, is shown in Fig. 3 for GaP and BTO samples. One can see that the modulation depth linearly depends on the vibration amplitude if the amplitude is smaller than the aver-

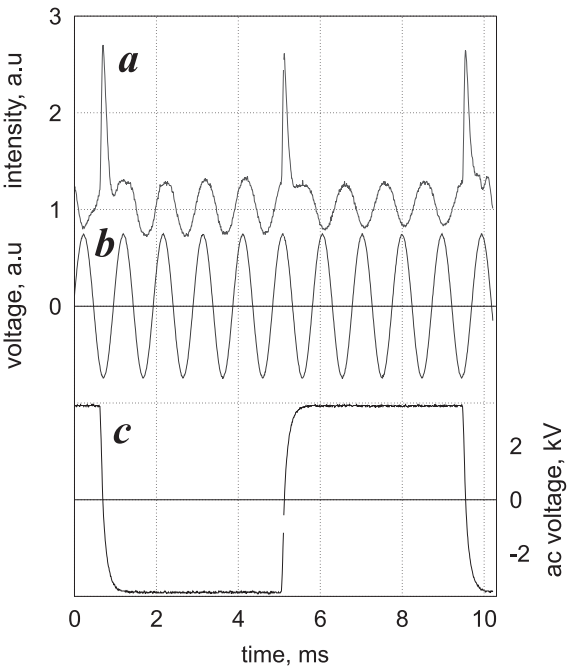

Fig. 2. Oscilloscope traces for (a) intensity modulation measured by the photodiode, (b) voltage applied to the piezo-driver, and (c) external voltage applied to the GaP sample. All traces were recorded simultaneously. Amplitude of the speckle pattern vibration is 0.45 μm and the average speckle size is 3.7 μm. Sharp peaks of the curve (a) are caused by the finite slew rate of the external voltage

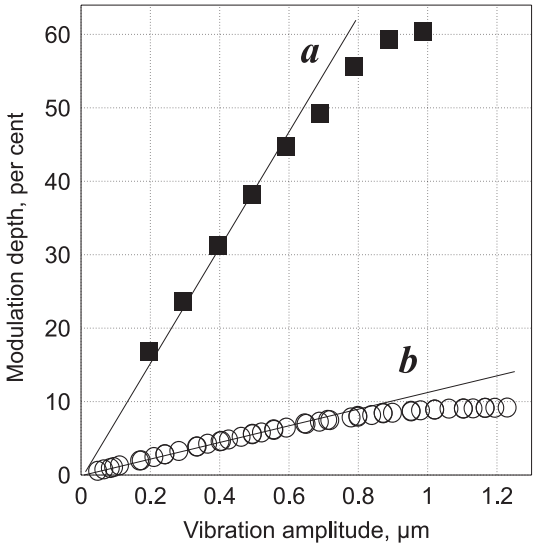

Fig. 3. Intensity modulation depth as a function of the speckle-pattern-vibration amplitude for (a) BTO and (b) GaP samples. *Solid lines* show the linear dependence on the vibration amplitude. The average speckle size is 3.0 μm for BTO and 3.7 μm for GaP. The modulation depth is defined as the ratio of the modulation amplitude to the average transmitted intensity

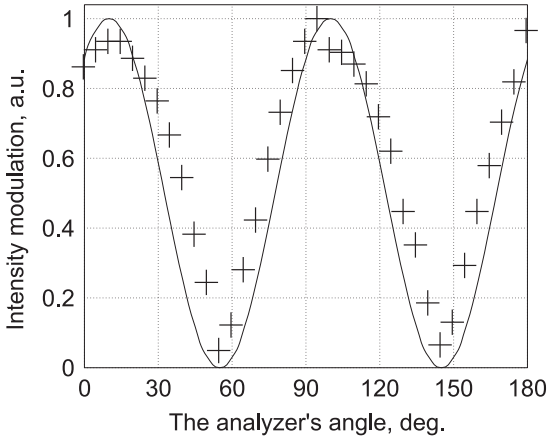

Fig. 4. Modulation amplitude as a function of the analyzer angle for the GaP crystal. Input polarization is perpendicular to the electric field vector. The vibration amplitude is 0.63 μm. External alternating voltage is ±3.4 kV at the repetition frequency of 85 Hz

age speckle size. When the speckle displacement becomes comparable with the mean speckle radius, the space-charge field recorded in the crystal is diminished due to effective broadening of the speckle size. The mechanism of this diminishing is similar to the interference-pattern-visibility decreasing during the recording of the time-averaged holographic interferogram. This is the reason of the deviation from the linear dependence for vibration amplitude larger than 0.6 μm. The intensity modulation depth obtained with the BTO sample is larger than for GaP which is probably caused by the larger electrooptic coefficient of BTO. We have checked that the modulation depth of the photodiode current does not depend on the input light power of the speckle pattern. The modulation depth varies within only 3% (which is inside the experimental error) whereas the intensity incident to the BTO crystal changes in the range of 1–20 $\mathrm{mW/cm^2}$.

1.2 Dependence of the intensity modulation on the polarization and applied voltage

The intensity-modulation amplitude is a function of the applied voltage, input polarization, and the analyzer's orientation. The input speckle pattern was linearly polarized in our experiments. Dependence of the intensity modulation amplitude on the analyzer angle, α, measured in respect to the applied electric field is shown in Fig. 4. Measurements were performed for the GaP sample in the case of the input polarization being perpendicular to the electric field. The experimental curve can be well fitted with the function $\cos^2(2\alpha + \Delta\alpha)$, where $\Delta\alpha$ is a fitting parameter equal to 10° for the particular curve shown in Fig. 4. For the GaP sample of the orientation shown in Fig. 1, we found four combinations of the input polarization and analyzer's orientation that yield the maximum intensity modulation. Optimum pairs of the input and output polarization are listed in Table 1, where the angles are measured with respect to the external electric field.

One can conclude from Table 1 that the optimum input polarization for the GaP sample is either close to the vertical or horizontal position and the analyzer is oriented either parallel or perpendicular to the input polarization state. The deviation from the exactly parallel (perpendicular) polarization state may stem from the non-exact orientation of the crystallographic axes of the sample cut. It was found that the optimum orientation of the input/output polarization does not depend on the external electric field for the GaP sample.

Dependence of the intensity modulation on the applied electric field for the GaP sample is shown in Fig. 5. The modulation amplitude reaches its maximum at a certain voltage and then falls down. At small voltages, the modulation grows proportionally to the square of the external electric field.

For the BTO sample the orientation dependence has a more complicated character because it is affected by the natural optical activity ($\rho = 6.5\,\mathrm{deg/mm}$ at $\lambda = 633\,\mathrm{nm}$) of this crystal. Here the optimum orientation of the polarization analyzer depends on the applied voltage for any input polarization. As an illustration, the analyzer orientation needed to achieve the maximum modulation amplitude is shown in Fig. 6 as a function of the applied voltage. During the measurement the input polarization of the speckle pattern was fixed along the external electric field, which is parallel to the axis $[\bar{1}11]$ in the BTO sample. Solid lines in Figs. 5 and 6 are the theoretical estimations that we discuss in Sect. 2.

Table 1. Input polarization and output analyzer position needed to get the maximum intensity modulation for the GaP sample

Input polarization /°	Output analyzer /°	Intensity modulation amplitude /mV
10	100	12.6
5	10	11.9
100	10	9.6
100	95	10.3

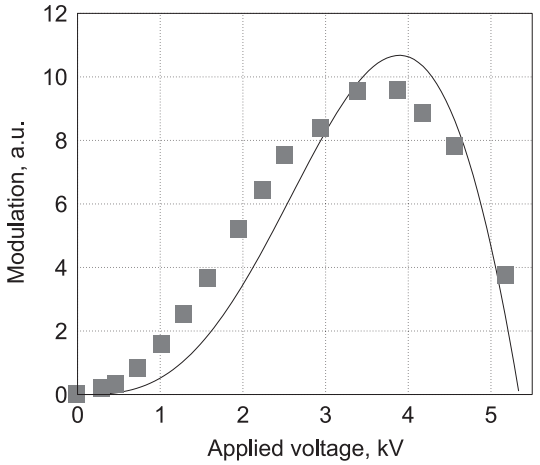

Fig. 5. Modulation amplitude as a function of applied external voltage for the GaP sample. *Solid line* is the theoretical estimation and *points* are measured values. The speckle pattern oscillates at the frequency 2 kHz with the amplitude of 0.63 μm

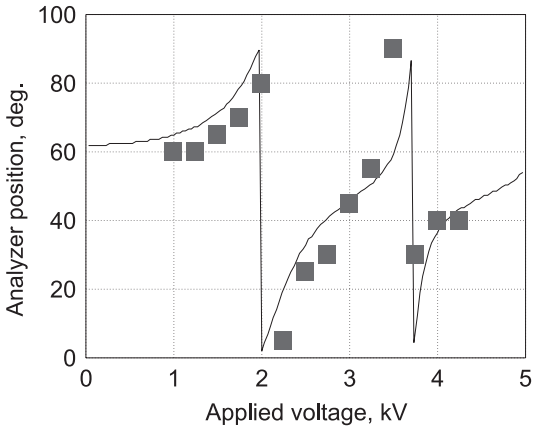

Fig. 6. The angle of the analyzer needed to obtain the maximal intensity-modulation-amplitude as a function of the applied external voltage for BTO crystal. *Solid line* is the theoretical estimation and points are the measured values. Polarization of the speckle pattern on the input face of the crystal is parallel to the applied electric field vector

1.3 Response time and adaptive property

According to the essence of the polarization self-modulation effect, the polarization state of the transmitted light is modulated only when the replica of the input intensity distribution is recorded inside the photorefractive crystal in the form of the space-charge distribution [12]. This space-charge could not be created immediately after the illumination of the crystal by a speckle pattern. A certain time is needed for charge carriers to be transported and re-trapped until the space-charge field reaches its steady state. The response time of the space-charge-field formation is defined by the material parameters of the crystal and by the intensity of the speckle pattern. Therefore, the intensity modulation amplitude in our experiment is expected to grow to the saturation level with time after switching the light on. This fact was confirmed experimentally. Additionally, it was found that the evolution of the intensity modulation does not change if we previously illuminate the sample by a vibrating speckle pattern and then switch the alternating electric field on at the moment $t = 0$. Figure 7 shows typical evolution of the intensity modulation amplitude for the BTO sample (Fig. 7a) and for the GaP sample (Fig. 7b). Note that the average intensity of the speckle pattern is 0.40 mW/cm^2 for the GaP crystal and 41 mW/cm^2 for BTO. GaP crystal exhibits faster response times owing to the higher mobility of charge carriers. Both curves in Fig. 7 can be well fitted by the usual exponential law:

$$I_{\mathrm{M}} = I_{\mathrm{ST}} \left[1 - \exp\left(-\frac{t}{\tau_{\mathrm{R}}} \right) \right] , \qquad (1)$$

where I_{ST} is the intensity modulation in the steady state and τ_{R} is the response time. It is worth noting that the signal dynamic described by (1) is different from the photorefractive process involving light diffraction, where the term in the square brackets is typically in the power of two. Direct comparison of the response time of the intensity modulation with that of the fanning effect carried out with the same intensity (41 mW/cm^2) and applied voltage (3 kV) in the BTO crystal reveals that the fanning effect is much slower: 3.0 s against 0.55 s. Therefore, we conclude that the observed modulation is not caused by the fanning effect.

Dependence of the response time on the speckle pattern intensity is shown in Fig. 8. It is seen that the response time is inversely proportional to the input intensity. In accordance with usual behavior of the space-charge formation, its response time is inversely proportional to the light inten-

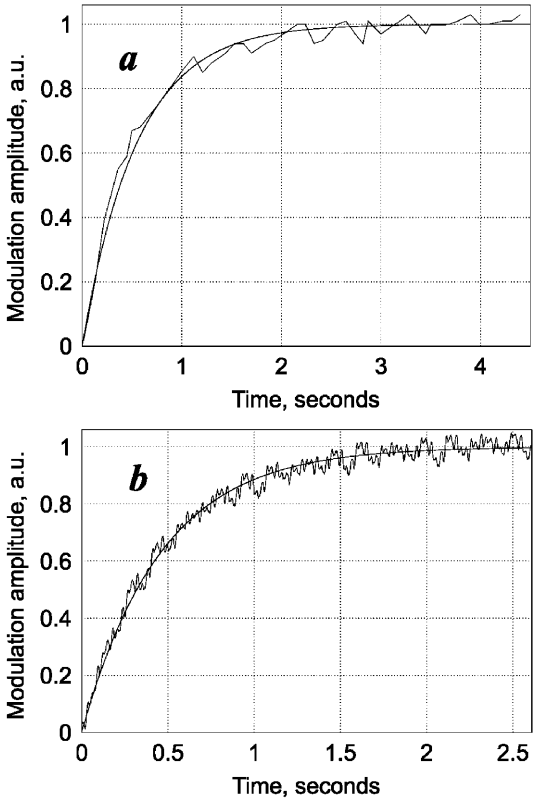

Fig. 7a,b. Temporal evolution of the intensity-modulation amplitude after switching the external voltage on for **a** BTO and **b** GaP crystals. The *regular lines* are the theoretical curves (1) and the *noisy lines* are the experimental data. The best fitting gives the response time $\tau_{\mathrm{R}} = 0.55$ s for BTO and $\tau_{\mathrm{R}} = 0.46$ s for GaP. The intensity of the speckle pattern incident in the crystal is 41 mW/cm^2 for BTO and 0.40 mW/cm^2 for GaP

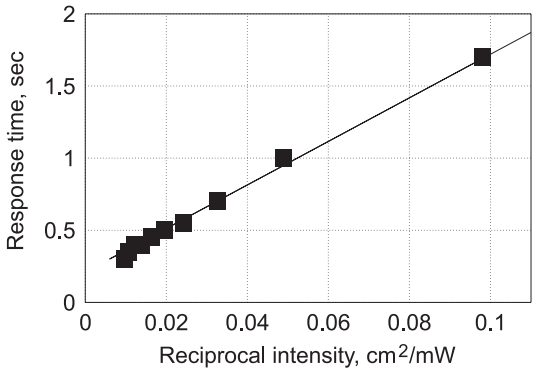

Fig. 8. The dependence of the intensity modulation's response time on the incident intensity of the speckle pattern for BTO crystal. Experimental data are shown as the points and the *solid line* illustrates that the response time is inversely proportional to the intensity of the speckle pattern

sity [13]. The response of the intensity modulation in our experiments also follows this rule as one can see in Fig. 8. Formation of the space-charge field replica of the speckle pattern means the recording of a spatial filter correlated with the input intensity distribution. Redistribution of the space charge in a photorefractive crystal is a reversible process with the characteristic time τ_R. Therefore, if a strong modification of the speckle pattern is introduced in the measurement system (for example, by change of the scattering object), the old correlation filter will be erased and a new one matched with the changed intensity distribution will be recorded. Consequently, the transmitted intensity will be modulated only when the time scale of speckle pattern variations is faster than τ_R. Otherwise, all slower changes (with $\tau > \tau_R$) do not modulate the polarization state of the transmitted light. In other words, such correlation filter possesses the property to be adaptive to slow environmental variations. Therefore, high long-term stability of the measured signal can be achieved. This property was experimentally verified for both photorefractive crystals: the intensity modulation depth is the same during 8 h of the measurements. If any strong disturbance is introduced in the setup, the same level of the signal is recovered after τ_R. High sensitivity of GaP can provide the response time of few ms at the moderate intensity level of 100 mW/cm^2, which is enough for many practical applications.

In our experiments we have found that the intensity modulation does not depend within the experimental error on the speckle-pattern vibration frequency from 100 Hz to 20 kHz (20 kHz is the highest excitation frequency of our particular piezo-driver.

2 Simplified theoretical model

A speckle pattern created by a coherent light beam scattered from a rough surface usually has a well-defined spatial structure with visibility about the unit providing separation of the illuminated areas by the areas of zero intensity [14]. Therefore, as an approximation, we consider here the speckle pattern consists of a set of Gaussian beams, whose diameters are normally distributed around the diameter equal to the average speckle size. When an optical system is used to collect the light into the crystal, the average speckle size w_0 in the transverse direction can be estimated as [15]:

$$w_0 = \frac{1.22\lambda}{\alpha}\,, \tag{2}$$

where λ is the light wavelength and α is the angle formed by a point at the input crystal surface and the effective aperture of the optical system. The average longitudinal size of the speckle in the direction of the light propagation in the medium with the refractive index n_0 is

$$s_z = \frac{4\lambda n_0}{\alpha^2}\,, \tag{3}$$

To describe the main features of the speckle pattern propagation, we will consider first the propagation of one Gaussian beam through the photorefractive crystal. It is well known that there are two different mechanisms (diffusion and drift) of the space-charge formation in photorefractive crystals. In the case of sinusoidal grating recording, the diffusion mechanism leads to the formation of the space-charge electric field, which is 90°-phase-shifted from the initial intensity distribution [16]. The diffusion recording occurs in crystals without external electric field because of diffusion of the light-induced charge carriers. Alternatively, the drift mechanism (strong dc external field is applied to the crystal) results in the formation of the space-charge field out of phase with the initial intensity distribution. The diffusion type of the photorefractive recording can be also achieved when the alternating electric field is applied to the crystal providing that its repetition period is much shorter than the specific recording time of the crystal [17]. The latter mechanism is known to be the most effective for fast photorefractive crystals such as sillenite crystals ($Bi_{12}SiO_{20}$ and $Bi_{12}TiO_{20}$) and semiconductors (GaAs and CdTe). In this paper we limit our consideration to the case of the enhanced diffusion recording in photorefractive crystals under external ac electric field of the square-wave form.

The intensity of the Gaussian beam depends on the transverse coordinate, therefore, such a beam will create a space-charge electric field while propagating through the photorefractive crystal. This electric field can be calculated by using the method proposed by Feinberg [18]. In the first step, the intensity distribution is expanded into the Fourier spectrum. Second, the space-charge field is calculated for each spatial frequency, and finally, the induced electric field is composed by the inverse Fourier transform. The input intensity distribution has the Gaussian shape:

$$I(x) = I_0 \exp\left(-\frac{4x^2}{w_0^2}\right)\,. \tag{4}$$

Here the one-dimensional case is considered taking into account that the space-charge field along the external electric field is much stronger than in the perpendicular direction. Expansion of (4) into the Fourier series allows us to calculate the visibility of the input interference pattern m_K as a function of the spatial frequency K:

$$m_K = \frac{2I_K\,\mathrm{d}K}{\int_{-\infty}^{\infty} I_K\,\mathrm{d}K} = I_0 w_0\,\mathrm{d}K \exp\left(-\frac{K^2}{K_0^2}\right)\,, \tag{5}$$

where I_K is the spectral component of the intensity at the spatial frequency K and $K_0 = 2/w_0$ is the boundary spatial

frequency of the Gaussian beam. In the next step, we calculate the space-charge electric field for each spatial frequency. Theory of the hologram recording in the photorefractive crystals under alternating electric field was developed by Stepanov and Petrov [13, 17]. They used an approximation of the small visibility ($m \ll 1$) and neglected the higher spatial harmonics. Under these approximations and using averaging over the external-field period, the space-charge field, E_{SC}, is expressed as [13]

$$\frac{\partial E_{SC}}{\partial t} = -\left(\frac{\mathrm{i}m_K \left[E_D(1+K^2 r_D^2) + K r_E E_A \right]}{\tau_M \left[(1+K^2 r_D^2)^2 + K^2 r_E^2 \right]} + \frac{E_{SC} \left[(1+K^2 r_D^2)(1+k^2 l_S^2) + K^2 r_E l_E \right]}{\tau_M \left[(1+K^2 r_D^2)^2 + K^2 r_E^2 \right]} \right) . \quad (6)$$

Here τ_M is the Maxwell relaxation time, E_D is the diffusion field, E_A is the amplitude of the external alternating field, r_E is the drift length, r_D is the diffusion length, l_S is the Debye screening length, and l_E is the electron tightening length by the electric field E_A. The parameters in (6) are expressed using the microscopic parameters of the crystal:

$$E_D = K\frac{D}{\mu} = K\frac{k_B T}{e} ; \tau_M = \frac{\varepsilon\varepsilon_0}{e\mu\tau}\frac{h\nu}{\alpha\beta I_0} ;$$
$$r_E = \mu\tau E_A ; \qquad r_D = \sqrt{D\tau} ;$$
$$l_S = \sqrt{\frac{\varepsilon\varepsilon_0 k_B T}{e^2 N_A}} ; \qquad l_E = \frac{\varepsilon\varepsilon_0 E_A}{e N_A} , \quad (7)$$

where e is the electron charge, k_B is the Boltzman constant, T is the temperature, $\varepsilon\varepsilon_0$ is the dielectric constant of the crystal, D is the diffusion coefficient, τ is the charge carrier's lifetime, μ is its mobility, N_A is the acceptors concentration, α is the absorption coefficient, β is the quantum efficiency, and $h\nu$ is the energy of the light quantum. For a Gaussian beam, the approximation of small input visibility $m_K \ll 1$ is usually valid. Moreover, if the typical average size of the speckle is few micrometers and the applied electric field is more than 1 kV/cm, we can simplify (6) considering the material parameters of BTO and GaP. For both crystals under the strong electric field, r_E exceeds other characteristic lengths: $r_E \gg r_D, l_S, l_E$. Therefore,

$$\frac{\partial E_{SC}}{\partial t} = -\frac{\mathrm{i}m_K E_A K r_E + E_{SC}}{\tau_M} . \quad (8)$$

This equation has simple analytical solution. Taking into account (5) and performing inverse Fourier transform, we can calculate the distribution of the induced space charge field:

$$E_{SC}(x,t) = \frac{4\mu\tau}{\sqrt{2\pi}}\frac{E_A^2}{w_0^2} x \exp\left(-\frac{4x^2}{w_0^2}\right)\left[1 - \exp\left(-\frac{t}{\tau_M}\right)\right] . \quad (9)$$

One can see that the space-charge field of the Gaussian beam is proportional to a gradient of the initial intensity distribution. Consequently, the light beam propagates in the self-induced, spatially non-uniform electric field, which is the sum of the space-charge field and the external field. The central part of the beam propagates in the field equal to the applied field, but the side parts are affected by either smaller or higher field. Owing to the linear electrooptic effect of a photorefractive crystal, the polarization state of the transmitted beam is a function of the x coordinate. By placing an analyzer behind the crystal, the polarization modulation is transformed into the intensity modulation. The transmission of the crystal–analyzer pair depends on the input/output polarization and crystal orientation. Let us consider the GaP crystal of the orientation used in the experiment. For any applied voltage in this case, the polarization eigenmodes are linear and have the angle of $\pm 45°$ with the external electric field. When the input polarization state is either parallel or perpendicular to electric field cubic, both polarization eigenmodes are excited equally. Therefore, if a quarter-wave voltage is applied to the sample, the central part of the transmitted beam is circularly polarized, while the right side of the beam is elliptically polarized with the longer axis parallel to the electric field as is schematically shown in Fig. 9. It is evident that the left part of the beam transmitted through the analyzer orientated parallel to the electric field will have much smaller intensity then the right part. The crystal–analyzer transmission is the even function of the total electric field and for this orientation it can be written as

$$T(x) = \cos^2\left(\frac{\pi n_0^3 r_{41}(E_A + E_{SC})L}{\lambda}\right) , \quad (10)$$

where λ is the light wavelength, n_0 is the refractive index of the crystal, r_{41} is its electrooptic coefficient, and L is the crystal's length. Therefore, the transmission will be different for the positive and negative semi-cycle of the applied electric field as shown in Fig. 10 assuming that the quarter-wave voltage is applied to the crystal. In both cases, the intensity of the transmitted beam is asymmetric function of the x coordinate. Analysis of (10) shows that the transmission is a symmetric function in respect to $x = 0$ (Fig. 10c) if no external field is applied to the crystal but the space charge field does exist. Transmission at $x = 0$ (which always corresponds to E_A) can

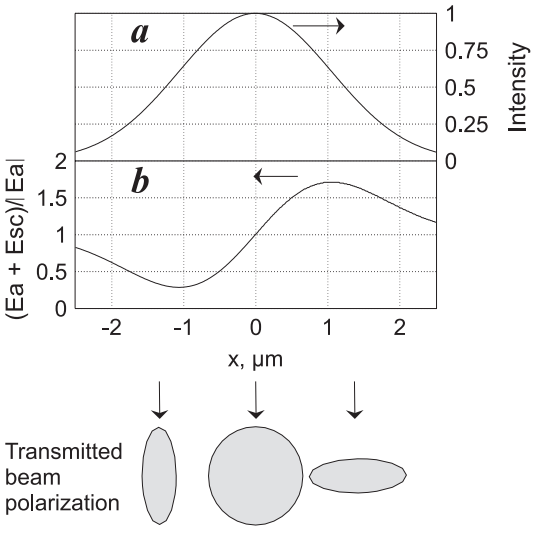

Fig. 9. Intensity distribution of a Gaussian beam with the beam diameter $w_0 = 3.0$ μm (a) and the total electric field inside the crystal in the steady state normalized to the applied field. The *lower part* of the figure shows the polarization state of the transmitted light when the quarter-wave voltage is applied to the crystal

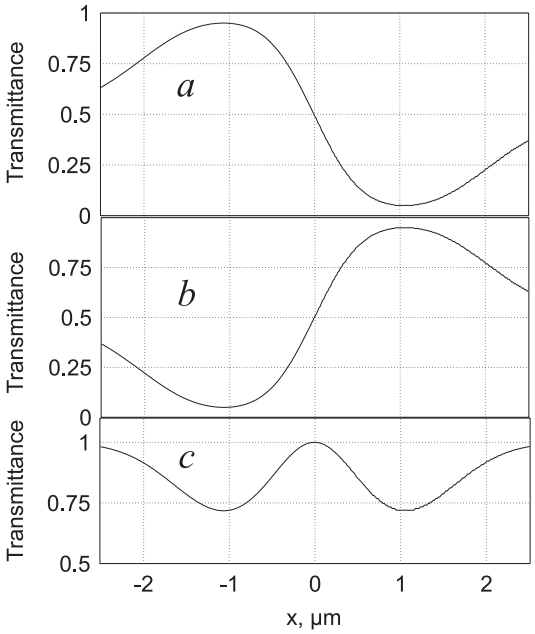

Fig. 10. The crystal-analyzer transmission: (a) during the positive semi-cycle of the applied voltage equal to the quarter-wave voltage, (b) during the negative semi-cycle of the same voltage, and (c) without applied voltage. The steady-state space-charge field created by the Gaussian beam ($w_0 = 3.0\,\mu$m) is the same in all cases

be considered as a working point around which the electric field is modulated. Any displacement of the incident beam position results in immediate change of its polarization state if the specific time of this displacement is shorter than the response time τ_R of the space-charge formation. Consequently, the polarization analyzer transforms this change into the intensity change.

It is clear from Fig. 10 that a small displacement of the incident beam from its average position ($x = 0$) is linearly transformed into intensity modulation only if the electric field is applied to the crystal. Therefore, harmonic oscillation of the incident beam at frequency Ω results in the intensity modulation at the same frequency. Comparing curves (a) and (b) in Fig. 10, one can conclude that there is π phase shift between the intensity modulation during the positive and negative semi-cycle. The same phase shift was observed in the experiment (see Fig. 2). For both semi-cycles, the modulation amplitude A_M is proportional to the gradient of the space-charge field at $x = 0$ but with the opposite sign. Only small modulation at the frequency 2Ω can be observed without external electric field.

Taking into account that all transmitted light is collected into the photodiode, the intensity I_Δ of the transmitted beam, displaced on the distance Δ, is proportional to the integral

$$I_\Delta = \int_{-\infty}^{\infty} I(x, \Delta) T(x)\,\mathrm{d}x\,, \quad \text{where}$$

$$I(x, \Delta) = I_0 \exp\left(-\frac{4(x-\Delta)^2}{w_0^2}\right)\,. \tag{11}$$

Figure 11 shows the dependence of the transmitted beam intensity on the beam displacement (curve a) in comparison

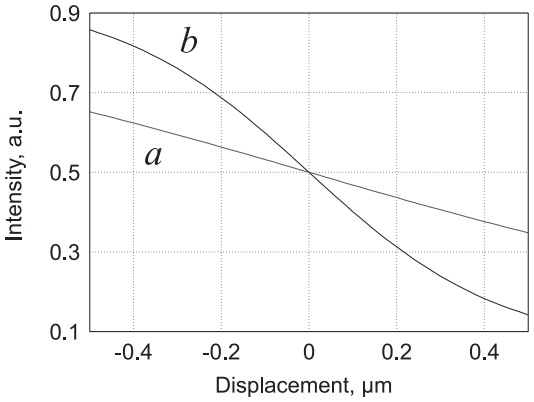

Fig. 11. (a) Intensity of the Gaussian beam transmitted through the photorefractive crystal and the polarization analyzer as a function of the beam displacement calculated using (11). (b) Dependence of the crystal–analyzer intensity transmission on the coordinate (10). The space-charge field created by the Gaussian beam of 3.0 μm is in the steady state

with the crystal–analyzer transmission (curve b). The latter curve is the middle part of the curve a in Fig. 10. One can see that accounting for the limited size of the propagating beam leads to a wider linear band of the response than could be suggested from the direct analysis of (10). Anyway, for small displacements, the integration of (11) introduces just an additional coefficient between intensity modulation and the gradient of the total electric field.

3 Discussion

One can see from (9)–(11) that both the space-charge field and the crystal–analyzer transmission do not depend on the Gaussian beam intensity, if the dark conductivity of the crystal is much smaller than the light-induced photoconductivity. Therefore, the modulation depth does not depend on the intensity either. It is very important for consideration of the speckle-pattern displacement in which the intensity of each speckle differs from one another. However, the modulation depth will be nearly the same for the all speckles if the speckle pattern's displacement is homogeneous. The latter condition is satisfied if the laser beam is reflected or refracted from a diffusely scattering object [19]. Then the modulation depth of the total intensity of all speckles collected by a lens into a photodiode is suggested to be the same as for one speckle of the mean size. In fact, formation of the space-charge field for each speckle means recording of the spatial filter, which correlates with the intensity distribution of the speckle pattern. The principal feature of this filter is that its transmission is proportional to the input intensity gradient providing linear transformation of the displacement into the intensity. The model of single-beam propagation explains the main features of the experiment with the oscillating speckle pattern. Particularly, the orientation dependencies are completely explained if we consider just propagation of the polarized light through the electrooptic crystal without taking into account light diffraction. The theoretical analysis of the previous section predicts same optimal combinations of the input/output polarization state for GaP sample as was observed in the experiment (Table 1). Solid lines in Figs. 4 and 6 are theoretical curves calculated for our par-

ticular samples GaP and BTO, respectively. Natural optical activity, piezoelectric and elasto-optic effects were considered when the optimal orientation of BTO was calculating (Fig. 6). We have used the same piezoelectric and elasto-optic coefficients for BTO as in [20]. Other BTO parameters used in numerical simulations are $r_{41} = 4.75\,\mathrm{pm/V}$, $n_0 = 2.58$, and $\rho = 6.5\,\mathrm{deg/mm}$.

The dependence of the intensity modulation on the external electric field can be calculated using (9)–(11). For GaP the theoretical curve is shown by the solid line in Fig. 5. To calculate this dependence, parameters of GaP reported in the literature ($r_{41} = 1.07\,\mathrm{pm/V}$, $n_0 = 3.45$, $\mu\tau = 1.7 \times 10^{-8}\,\mathrm{cm^2/V}$) were used [21]. Equation (10) includes also the parameter L, which is the interaction length of the light with the crystal. It was found that the best agreement of the theory with the experiment is achieved for $L = 6.8\,\mathrm{mm}$, which is shorter than the crystal length (10 mm). However, it is much longer than the mean longitudinal speckle size equal to 130 μm according to (3). Therefore, we can assume that the intensity modulation arisen from the individual speckle recording is summarized with some statistical coefficients in the direction of light propagation as well.

It should be noted that the linearized model of the space-charge formation is valid only when the average speckle size is smaller than the drift length r_E, which is proportional to the external field E_A (7). In that case, the higher spatial harmonics of the space-charge field can be neglected [22]. When the stronger electric field is applied to the crystal, the gradient $\mathrm{d}E_\mathrm{SC}/\mathrm{d}x|_{x=0}$ rigorously calculated using nonlinear equations [22] is higher than the estimations obtained with the linearized theory. This must affect the modulation intensity of the transmitted speckle pattern. Our GaP sample has a relatively large inter-electrode distance that does not allow application of a strong electric field. Therefore, the experiment is qualitatively explained by the linear theory. However, for a thinner BTO sample in which larger r_E can be obtained, the linear theory fails to explain the dependence of the intensity modulation on the applied electric field.

It is seen from (9) that the gradient $\mathrm{d}E_\mathrm{SC}/\mathrm{d}x|_{x=0}$ increases linearly in time after switching the external field on. The response time of this process is equal to the Maxwell relaxation time, τ_M. Note that τ_M is the fastest response time corresponding to the space-charge-grating formation at zero spatial frequency [13]. Higher spatial frequencies (for example of the fanning gratings) are created much more slowly. The intensity modulation in our experiment is proportional to the gradient $\mathrm{d}E_\mathrm{SC}/\mathrm{d}x|_{x=0}$ if the quarter-wave field is applied to the crystal. Therefore, the intensity modulation also grows linearly in time as was observed in the experiment (Fig. 7). Proportionality of the intensity-modulation response time to the reciprocal intensity is evident from (7), which describes τ_M.

4 Conclusions

A simple theoretical model of the polarization self-modulation effect based on the Gaussian beam propagation through the photorefractive crystal explains the main features of the experiment with oscillating speckle-pattern. It is shown that the linear transformation of the speckle-pattern displacement into the intensity modulation is achieved in photorefractive crystals of GaP and $Bi_{12}TiO_{20}$. Immediate response of the system ensures the measurements of non-periodic displacement of the speckle-pattern as well. Owing to the gradient type of the spatial filter recorded in the crystal, the sensitivity of the method is as high as for an interferometer. In contrast with an interferometer, the proposed optical system is very simple and self-referenced: information about the speckle pattern displacement is optically reconstructed by the speckle pattern itself. The ability of a photorefractive crystal to re-record the space-charge distribution makes the system adaptive to slowly varying environmental conditions. The response time of few ms can be achieved in semi-insulating GaP crystal under a moderate intensity of the input speckle pattern. Therefore, highly precise measurements can be carried out with this crystal without any vibro-isolated table. Moreover, this crystal is sensitive in the in the spectral region from 0.6 to 0.9 μm. Therefore, semiconductor lasers can be used as a light source allowing us to design compact optical sensors. The proposed method can be also used as a simple instrument for the measurement of material parameters of the photorefractive crystals.

Acknowledgements. The authors acknowledge Dr. A.V. Khomenko for useful discussions. The authors from Finland appreciate the financial support of the Academy of Finland.

References

1. T.J. Hall, M.A. Fiddy, M.S. Ner: Opt. Lett. **5**, 485 (1980)
2. A.A. Kamshilin, M.P. Petrov: Opt. Commun. **53**, 23 (1985)
3. S.I. Stepanov: In *International Trends in Optics* (Academic Press, Boston, San Diego 1991) p. 125
4. R.K. Ing, J. Monchalin: Appl. Phys. Lett. **59**, 3233 (1991)
5. H.J. Tiziani, J. Klenk: Appl. Opt. **20**, 1467 (1981)
6. K. Nakagava, T. Minemoto: Opt. Commun. **70**, 288 (1989)
7. N.A. Korneev, S.I. Stepanov: Optik **91**, 61 (1992)
8. A.A. Kamshilin, T. Jaaskelainen, A.V. Khomenko, A. Garcia-Weidner: Appl. Phys. Lett. **67**, 2585 (1995)
9. A.A. Kamshilin, E. Raita, K. Paivasaari, T. Jaaskelainen, Y.N. Kulchin: Appl. Phys. Lett. **73**, 1466 (1998)
10. M.P. Petrov, S.I. Stepanov, G.S. Trofimov: Sov. Tech. Phys. Lett. **12**, 379 (1986)
11. N.A. Korneev, S.I. Stepanov: Opt. Commun. **115**, 35 (1995)
12. A.A. Kamshilin, A.V. Khomenko, C.A. Fuentes-Hernandez, K. Paivasaari: submitted to Opt. Lett. (1998)
13. S.I. Stepanov, M.P. Petrov: In *Photorefractive Materials and their Applications I. Fundamental Phenomena* (Springer, Berlin, Heidelberg 1988) p. 263
14. B.Y. Zeldovich, A.V. Mamaev, V.V. Shkunov: *Speckle-wave Interactions in Application to Holography and Nonlinear Optics* (CRC Press, Boca Raton 1995)
15. I. Yamaguchi: In *Speckle Metrology* (Marcel Dekker, New York 1993) p. 1
16. N.V. Kukhtarev, V.B. Markov, S.G. Odulov, M.S. Soskin, V.L. Vinetskii: Ferroelectrics **22**, 961 (1979)
17. S.I. Stepanov, M.P. Petrov: Opt. Commun. **53**, 292 (1985)
18. J. Feinberg: J. Opt. Soc. Am. **72**, 46 (1982)
19. T. Asakura, N. Takai: Appl. Phys. **25**, 179 (1981)
20. S.I. Stepanov, S.M. Shandarov, N.D. Hat'kov: Sov. Phys. -Solid State **29**, 1754 (1987)
21. K. Kuroda, Y. Okazaki, T. Shimura, H. Okamura, M. Chihara, M. Itoh, I. Ogura: Opt. Lett. **15**, 1197 (1990)
22. S.M. Shandarov, N.I. Nazhestkina, O.V. Kobozev, A.A. Kamshilin: Appl. Phys. B **68**, 1007 (1999)